

Magnetic field modulation of intense surface plasmon polaritons

C. Clavero*,¹, K. Yang¹, J. R. Skuza², and R. A. Lukaszew^{1,2}

¹ Department of Applied Science, College of William & Mary, Williamsburg, Virginia 23187, USA.

² Department of Physics, College of William & Mary, Williamsburg, Virginia 23187, USA.

*cclavero@wm.edu

Abstract: We present correlated experimental and theoretical studies on the magnetic field modulation of Surface Plasmon Polaritons (SPPs) in Au/Co/Au trilayers. The trilayers were grown by sputter deposition on glass slides with the Co films placed at different distances from the surface and with different thickness. We show that it is possible to tailor Au/Co/Au trilayers with the critical thickness needed for optimum excitation of SPPs leading to large localized electromagnetic fields. The modification of the SPP wave vector by externally applied magnetic fields was investigated by measuring the magneto-optical activity in transverse configuration. In addition, using magneto-optics as a tool we determined the spatial distribution of the SPP generated electromagnetic fields within Au/Co/Au samples by analyzing the field-dependent optical response, demonstrating that it is possible to excite SPPs that exhibit large electromagnetic fields that are also magneto-optically active and therefore can be modulated by externally applied magnetic fields.

©2010 Optical Society of America

OCIS codes: (240.6680) Surface plasmons; (250.5403) Plasmonics; (160.3820) Magneto-optical materials; (230.3810) Magneto-optic systems; (280.4788) Optical sensing and sensors; (310.4165) Multilayer design.

References and links

1. H. Raether, "Surface Plasmons on Smooth and Rough Surfaces and on Gratings," Vol. 111 of Springer Tracts in Modern Physics (Springer-Verlag, Berlin, 1988).
2. S. S. Y. J. Homola, and G. Gauglitz, "Surface plasmon resonance sensors: review," *Sensors and Actuators B* **54**(1-2), 3–15 (1999).
3. T. Nikolajsen, K. Leosson, and S. I. Bozhevolnyi, "Surface plasmon polariton based modulators and switches operating at telecom wavelengths," *Appl. Phys. Lett.* **85**(24), 5833–5835 (2004).
4. W. L. Barnes, A. Dereux, and T. W. Ebbesen, "Surface plasmon subwavelength optics," *Nature* **424**(6950), 824–830 (2003).
5. Y. M. Strel'nik, and D. J. Bergman, "Optical transmission through metal films with a subwavelength hole array in the presence of a magnetic field," *Phys. Rev. B* **59**(20), R12763–R12766 (1999).
6. G. A. Wurtz, W. Hendren, R. Pollard, R. Atkinson, L. Le Guyader, A. Kirilyuk, T. Rasing, I. I. Smolyaninov, and A. V. Zayats, "Controlling optical transmission through magneto-plasmonic crystals with an external magnetic field," *N. J. Phys.* **10**(10), 105012 (2008).
7. Y.-C. Lan, Y.-C. Chang, and P.-H. Lee, "Manipulation of tunneling frequencies using magnetic fields for resonant tunneling effects of surface plasmons," *Appl. Phys. Lett.* **90**(17), 171114 (2007).
8. K. J. Chau, S. E. Irvine, and A. Y. Elezzabi, "A gigahertz surface magneto-plasmon optical modulator," *IEEE J. Quantum Electron.* **40**(5), 571–579 (2004).
9. J. B. Khurgin, "Optical isolating action in surface plasmon polaritons," *Appl. Phys. Lett.* **89**(25), 251115 (2006).
10. B. Sepúlveda, A. Calle, L. M. Lechuga, and G. Armelles, "Highly sensitive detection of biomolecules with the magneto-optic surface-plasmon-resonance sensor," *Opt. Lett.* **31**(8), 1085–1087 (2006).
11. M. S. Kushwaha, and P. Halevi, "Magnetoplasmons in thin films in the Voigt configuration," *Phys. Rev. B* **36**(11), 5960–5967 (1987).
12. P. E. Ferguson, O. M. Stafsudd, and R. F. Wallis, "Surface magnetoplasma waves in nickel," *Physica B+C*, **86–88**, 1403–1405 (1977).
13. P. E. Ferguson, O. M. Stafsudd, and R. F. Wallis, "Enhancement of the transverse Kerr magneto-optic effect by surface magnetoplasma waves," *Physica B+C* **89**, 91–94 (1977).
14. R. K. Hickernell, and D. Sarid, "Long-range surface magnetoplasmons in thin nickel films," *Opt. Lett.* **12**(8), 570–572 (1987).

15. J. J. Burke, G. I. Stegeman, and T. Tamir, "Surface-polariton-like waves guided by thin, lossy metal films," *Phys. Rev. B* **33**(8), 5186–5201 (1986).
16. R. Zia, M. D. Selker, and M. L. Brongersma, "Leaky and bound modes of surface plasmon waveguides," *Phys. Rev. B* **71**(16), 165431 (2005).
17. C. Hermann, V. A. Kosobukin, G. Lampel, J. Peretti, V. I. Safarov, and P. Bertrand, "Surface-enhanced magneto-optics in metallic multilayer films," *Phys. Rev. B* **64**(23), 235422 (2001).
18. J. B. González-Díaz, A. Garcia-Martin, G. Armelles, J. M. Garcia-Martin, C. Clavero, A. Cebollada, R. A. Lukaszew, J. R. Skuza, D. P. Kumah, and R. Clarke, "Surface-magnetoplasmon nonreciprocity effects in noble-metal/ferromagnetic heterostructures," *Phys. Rev. B* **76**(15), 153402 (2007).
19. V. I. Safarov, V. A. Kosobukin, C. Hermann, G. Lampel, J. Peretti, and C. Marlière, "Magneto-optical Effects Enhanced by Surface Plasmons in Metallic Multilayer Films," *Phys. Rev. Lett.* **73**(26), 3584–3587 (1994).
20. N. Bonod, R. Reinisch, E. Popov, and M. Nevière, "Optimization of surface-plasmon-enhanced magneto-optical effects," *J. Opt. Soc. Am. B* **21**(4), 791–797 (2004).
21. D. P. Kumah, A. Cebollada, C. Clavero, J. M. Garcia-Martin, J. R. Skuza, R. A. Lukaszew, and R. Clarke, "Optimizing the planar structure of (111) Au/Co/Au trilayers," *J. Phys. D Appl. Phys.* **40**(9), 2699–2704 (2007).
22. M. Schubert, "Polarization-dependent optical parameters of arbitrarily anisotropic homogeneous layered systems," *Phys. Rev. B* **53**(8), 4265–4274 (1996).
23. M. Schubert, T. E. Tiwald, and J. A. Woollam, "Explicit Solutions for the Optical Properties of Arbitrary Magneto-Optic Materials in Generalized Ellipsometry," *Appl. Opt.* **38**(1), 177–187 (1999).
24. E. D. Palik, "*Handbook of optical constants of solids*", Academic Press, Orlando (1985).
25. S. Park, X. Zhang, A. Misra, J. D. Thompson, M. R. Fitzsimmons, S. Lee, and C. M. Falco, "Tunable magnetic anisotropy of ultrathin Co layers," *Appl. Phys. Lett.* **86**(4), 042504 (2005).
26. D. Weller, J. Stöhr, R. Nakajima, A. Carl, M. G. Samant, C. Chappert, R. Mégy, P. Beauvillain, P. Veillet, and G. A. Held, "Microscopic origin of magnetic anisotropy in Au/Co/Au probed with x-ray magnetic circular dichroism," *Phys. Rev. Lett.* **75**(20), 3752–3755 (1995).
27. T. Koide, H. Miyauchi, J. Okamoto, T. Shidara, A. Fujimori, H. Fukutani, K. Amemiya, H. Takeshita, S. Yuasa, T. Katayama, and Y. Suzuki, "Direct determination of interfacial magnetic moments with a magnetic phase transition in Co nanoclusters on Au(111)," *Phys. Rev. Lett.* **87**(25), 257201 (2001).
28. P. Bertrand, C. Hermann, G. Lampel, J. Peretti, and V. I. Safarov, "General analytical treatment of optics in layered structures: Application to magneto-optics," *Phys. Rev. B* **64**(23), 235421 (2001).

1. Introduction

Surface plasmon polaritons (SPPs) are transverse magnetic (TM) surface waves propagating along the interface between two materials with dielectric constants of opposite sign, generally a metal and a dielectric [1]. They result from the interactions between an illuminating wave and the free electrons of the conductor, generating highly confined electromagnetic (EM) fields at the interface. SPPs have been extensively studied and used in a number of applications, including biosensors [2], optical modulators and switches [3], and new generation plasmonic devices [4]. SPP technology is an attractive platform for the development of nanoscale optical integrated circuits with passive and active devices, achieving and controlling light propagation in sub-wavelength geometries [4]. Thus, the control of SPPs by external magnetic fields has led to striking results, such as the manipulation of optical transmission through magneto-plasmonic crystals with external magnetic fields [5,6] or the control of terahertz SPPs on semiconductor surfaces by applying an external static magnetic field [7]. As a consequence, a number of technological applications have appeared in the last few years, including magneto-plasmonic optical modulators [8], optical isolators [9] and magneto-plasmonic sensors [10]. Nevertheless, for many applications it is important to achieve high intensity SPPs that also exhibit strong dependence on externally applied magnetic fields.

Previous reports have indicated that the SPP dispersion relation can be affected by applying magnetic fields perpendicular to the propagation vector of the SPP and along the surface, *i.e.* in the so called transverse configuration [11], in single layered magnetic materials [12,13], giving rise to field-dependent variations of the SPP wave vector k_{sp} . This effect has been observed for bounded SPP modes in which the electromagnetic field generated by the SPPs in the metallic film decays exponentially in the surrounding dielectric films [14] and for symmetric leaky SPP modes in which the electromagnetic field decays in the dielectric with lower refractive index and radiates towards the dielectric of higher refractive index [12,13] [Fig. 1(a)]. The leaky modes are of special interest, since they generate very intense localized EM fields, and thus they are very sensitive to the interface conditions, giving rise to applications as sensors and for signal transmission in integrated circuits. These modes can be

excited in the Kretschmann configuration [15,16], where the metallic films are optically coupled to a prism and far-field light is angled through the prism such that the in-plane wave vector $k_{||}=k_0 n_{prism} \sin\theta$ matches the associated SPP propagation constant k_{sp} [Fig. 1(a)], where $k_0=\omega/c$ is the wave number in vacuum, θ is the incidence angle and n_{prism} is the refractive index of the prism. Unlike the bounded modes, these modes lose energy not only due to the inherent absorption inside the metal, but also due to leakage radiation emitted into the prism. Thus, in the Kretschmann configuration a minimum in the reflected intensity is obtained at a critical incidence angle θ_c due to destructive interference between the leakage radiation emitted by the excited SPPs and the incoming light at the boundary with the prism [1]. This minimum actually vanishes for a critical metal thickness d_c , associated with optimum SPP excitation and thus leading to maximum EM fields. Such critical thickness depends strongly on the absorption losses of the metal. Thus, in this configuration and for magnetic metals, the variation of the SPP wave vector k_{sp} when an external magnetic field is applied [Fig. 1(b)] gives rise to a change of the SPP excitation condition and thus to a shift of the critical incidence angle θ_c . As a consequence, a strong field-dependent variation of the reflectivity is observed giving rise to a strong enhancement of the transverse magneto-optical Kerr effect (TMOKE) [12,13], [17,18]. Nevertheless, ferromagnetic metals such as Fe and Co have very high absorption losses compared to noble metals, i.e. Au and Ag, giving rise to overdamped SPP modes associated with low EM fields. Figure 1(b) shows the dispersion relation for the symmetric leaky SPP modes in Au and Co illuminated in the Kretschmann configuration using a quartz prism. Due to the high absorption of Co, the SPP dispersion relation is similar to that of light propagating through air. Combined noble-ferromagnetic systems have been proposed as Au/Co/Au trilayers [17–19], giving rise to a system with lower absorption losses and thus higher EM fields but still with sensitivity to external magnetic fields. In their studies, special attention was devoted to the large enhancement of the magneto-optical (MO) activity associated with the SPP excitation [17–20].

In the present studies, rather than optimizing the MO response, our attention was devoted to optimum excitation of SPPs, leading to maximization of the generated EM fields at the surface without compromising dependence with externally applied magnetic fields. To this end, Au/Co/Au trilayers were grown by sputter deposition on glass slides with the Co layers placed at different distances from the surface and with different thickness. We have been able to probe the SPP generated EM fields, and to demonstrate that it is experimentally possible to achieve optimal SPP excitation with strong dependence on external magnetic fields.

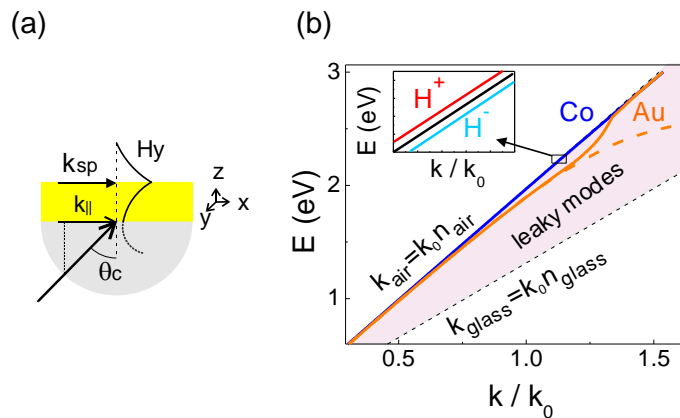


Fig. 1. (a) Schematic view of momentum matching in the Kretschmann configuration, where far-field radiation couples symmetric leaky SPP modes at the air-metal interface by means of a glass prism. H_y represents the only magnetic component in the TM mode. (b) Dispersion relation for such modes in Co and Au films considering their absorption losses. The dashed line shows the dispersion relation for Au considering no absorption losses. The dispersion relation of Co splits into two branches when external magnetic fields are applied along the y direction.

2. Experimental

Au/Co/Au trilayers were grown on soda-lime glass substrates via magnetron sputtering deposition in an ultra high vacuum (UHV) system under a base pressure in the low 10^{-9} Torr range. Slow deposition rates of 0.066 Å/s and 0.319 Å/s for Co and Au respectively allowed accurate thickness control. Soda-lime glass substrates, previously cleaned ultrasonically in successive baths of acetone and methanol, were UHV annealed at 600 °C for 30 minutes in order to planarize the surface [21]. Subsequently, a Au buffer layer was grown at RT and then annealed for 10 minutes at 350 °C in order to further planarize the Au surface before Co growth. Co films with thickness ranging from 2.5 to 10 nm were grown at 150 °C to favor surface diffusion of the incoming adatoms and thus give rise to a bi-dimensional growth mode with low interfacial roughness. Finally, a 3 nm thick Au capping layer was grown to prevent Co oxidation and to improve the generation and propagation of the SPPs on the upper metal-air interface. The thickness of the different layers was monitored using *ex-situ* x-ray reflectivity (XRR) carried out using a standard four-circle diffractometer with $Cu K\alpha$ radiation ($\lambda=1.5418$ Å) in the Bragg-Brentano configuration and with $1/32^\circ$ slits. Variable angle spectroscopic ellipsometry provided the actual optical constants for the Au and Co layers in the spectral range of 1.5 to 3 eV.

The optical and MO response of the multilayers under SPP excitation were investigated in the Kretschmann configuration using *p*-polarized He-Ne laser radiation ($\lambda=632.8$ nm). In this configuration [Fig. 1(a)], the glass substrate is coupled to a semicylindrical glass prism by a matching refractive index liquid. In our experimental setup the prism was mounted on an automated goniometer allowing illumination in total internal reflection with variable incidence angle θ and angular resolution of 10^{-4} degrees. A Si amplified photodetector preceded by a *p*-oriented polarizer was used to detect intensity variations in the reflected radiation. The TMOKE was also investigated by applying a 30 mT alternating magnetic field (60 Hz) in the plane of the sample and perpendicular to the incidence plane, intense enough to saturate the Co layers with in-plane magnetization. The TMOKE signal, i.e. the intensity variation of the *p*-polarized reflected light when applying magnetic fields in opposite directions $\Delta R_{pp}=R(+H)-R(-H)$, was detected and analyzed using lock-in techniques.

3. Results and discussion

Maximum SPP-generated EM fields are obtained when illuminating under the critical incidence angle θ_c and for a critical thickness d_c that depends strongly on the dielectric constants of the metal. Fig. 2 (a) shows reflectivity curves for Co and Au films for which the absorption losses are considerably different and thus their critical thicknesses d_c are 9.7 and 48.2 nm respectively. A much broader reflectivity curve is obtained for Co due to its higher absorption. For these particular thicknesses, maximum EM fields appear at the metal-air interface as shown in Fig. 2(b). Nevertheless, high absorption losses in Co drastically reduce the SPP-generated EM fields in this metal. On the other hand, Co films alone exhibit maximum TMOKE response ΔR_{pp} , as shown in Fig. 2(c). Thus, Au-Co multilayered systems are better suited to achieve SPPs with larger localized electromagnetic fields that can also be modulated by externally applied magnetic fields. Several factors have to be taken into account to accomplish this scenario, namely accurate control of the total thickness of the full trilayer, the thickness of the Co layer and its position within the film, as well as the discrepancy between the optical constants in very thin layers with respect to bulk values. In these studies the top Au layer thickness was minimized to 3 nm to allow the Co film to be as close as possible to the excited SPP thus making the trilayer system more sensitive to external magnetic fields. Fig. 2(d), (e) and (f) show the minimum value of the reflectivity R_{min} , the maximum value of the electromagnetic field $|H_y|_{max}$ and the maximum value of the MO activity ΔR_{max} for Au/Co/Au trilayers with each combination of Co and Au thicknesses calculated using transfer matrix formalism [22,23] and bulk optical constants [24] at 1.96 eV. The maximum intensity of the SPP generated H_y is obtained for single Au films and decays abruptly when Co is inserted in the structure as shown in Fig. 2(e). On the other hand, the

maximum TMOKE response ΔR is obtained for pure Co films, decreasing progressively when Au is inserted in the structure. Thus, in order to achieve large EM fields in the upper Au-air interface while keeping sensitivity to external magnetic fields it is necessary to minimize the Co layer thickness. Nevertheless, to maintain the integrity of the trilayer structure, the Co film needs to be thick enough to guarantee its continuity as a full layer. We have estimated that 3 nm is the minimum Co thickness that can yield a continuous Co layer when deposited on the Au buffer [21]. For such Co thickness, and considering a 3 nm thick Au capping layer mentioned previously, the maximum SPP generated EM field is obtained when the buffer layer is 20 nm thick so that the critical thickness is achieved, as shown in Fig. 2(e).

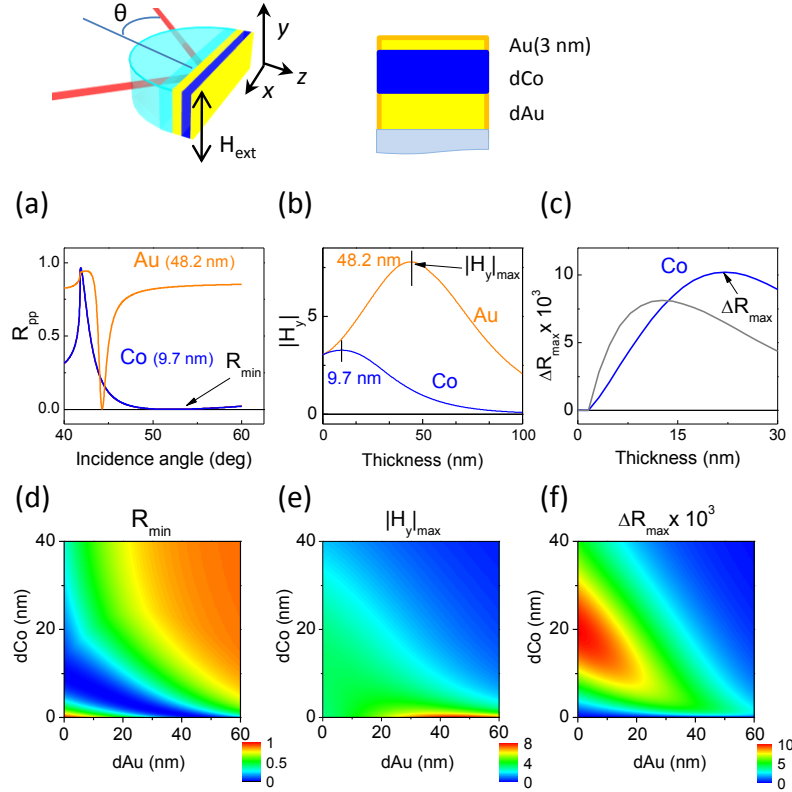


Fig. 2. Schematic view of the SPP excitation in the Kretschmann configuration for the Au(3nm)/Co(d_{Co})/Au(d_{Au}) trilayers where external magnetic field H_{ext} is applied along y . (a) Reflectivity curves calculated for Co and Au films with critical thickness, (b) SPPs $|H_y|$ at the metal-air interface for Co and Au films as a function of the thickness and (c) Transverse magneto-optical Kerr effect ΔR for a single Co film and for Au(3nm)/Co(d_{Co})/Au(20 nm) trilayers as a function of the Co thickness. The lower row represents calculations of (d) R_{min} , (e) $|H_y|_{max}$ and (f) ΔR_{max} for any combination of Au and Co thickness in the Au(3nm)/Co(d_{Co})/Au(d_{Au}) trilayers.

Nevertheless, due to the dependence of the optical constants with thickness in thin layers, the critical thickness might not be experimentally achieved for the predicted Au buffer and Co layer thickness. For this reason, a series of Au (3 nm)/Co (d_{Co})/Au (20 nm)/glass trilayer structures with different Co thickness from $d_{Co}=2.5$ to 10 nm was prepared. Figure 3(a) shows the angular dependency of the p -polarized reflectivity in the Kretschmann configuration R_{pp} for the different trilayers. Evidence of SPP excitation is the characteristic minimum observed in reflectivity around the resonance angle $\theta_R \sim 44.7^\circ$. A minimum reflectivity value as low as 1×10^{-5} was obtained for $d_{Co}=2.8$ nm. The inset in Figure 3(a) illustrates how critical the optimization of the Co layer thickness is to minimize the overall reflectivity of the sample.

Indeed, our experimental results show a good agreement with simulations using the transfer matrix formalism as shown in Fig. 3(b).

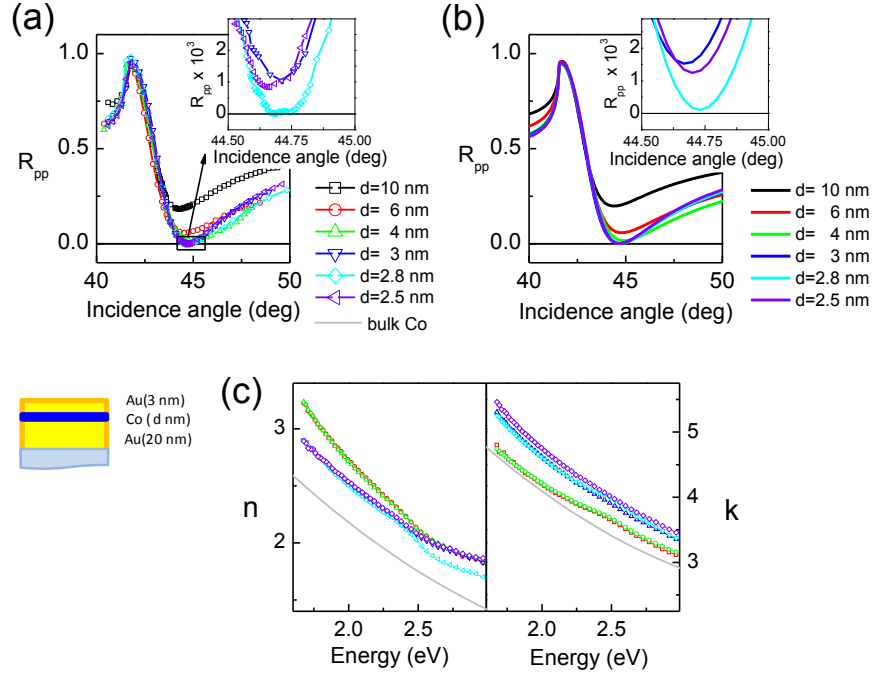


Fig. 3. (a) Experimental and (b) simulated angular dependency of the reflectivity with no external magnetic field applied R_{pp} for the Au(3 nm)/Co(d_{Co})/Au(20 nm) trilayers with d_{Co} ranging from 2.5 to 10 nm. (c) Real (n) and imaginary (k) parts of the complex refractive index of Co film measured with ellipsometry.

Interestingly, direct correlation of the Co optical constants with film thickness is observed [Fig. 3(c)]. We note that in previous studies, several other properties have also been reported to be Co-thickness dependent in Au/Co/Au trilayers, *e.g.* Co lattice parameter [21], magnetic anisotropy [25] or magnetic moment [26,27] to name a few. These changes are primarily due to the misfit between the Co and Au lattices and also due to confinement effects since the Co thickness approaches a monolayer. In the present case, we find a progressive decrease in the absorption coefficient k as the Co thickness increases approaching the bulk value, while n is nearly constant for all samples but slightly higher than bulk value.

In order to discuss the MO response of these trilayers, we recall that the shift observed in the position of the reflectivity minimum in magnetic materials is due to modification of the SPP wave vector by the external magnetic field. Figure 4(a) shows the angular dependency of the MO signal ΔR_{pp} for the Au(3 nm)/Co (d)/Au (20 nm)/glass trilayers with different Co thickness from $d=2.5$ to 10 nm, exhibiting a resonance-like feature associated with SPP excitation around θ_c for all the trilayers. In this case, a maximum value of $\Delta R_{pp}=7 \times 10^{-3}$ is obtained for the trilayer with Co thickness $d=10$ nm, decreasing for lower and higher Co thicknesses in agreement with the simulations in Fig. 2(c). The variation of the SPP wave vector $\Delta \mathbf{k}_{sp} = \mathbf{k}_{sp}(+H) - \mathbf{k}_{sp}(-H)$ when magnetic fields are applied in opposite directions along y was simulated using transfer matrix formalism [22,23], and imposing the boundary conditions characteristic of symmetric leaky SPP modes, *i.e.* an exponential decay of the EM field in the air-metal interface and an exponential increase at the lower Au-prism interface [15]. Figure 4(b) shows the calculated $\Delta \mathbf{k}_{sp}$ variation of the SPP k -vector for the Au(3 nm)/Co (d)/Au (20 nm)/glass trilayers with varying Co thickness from $d=2.5$ to 10 nm, where a maximum variation is obtained around the radiation energy used in our experiments (1.96 eV). In

addition, we observe that the variation of the SPP k -vector scales with the maximum value of the magneto-optical activity ΔR_{pp} .

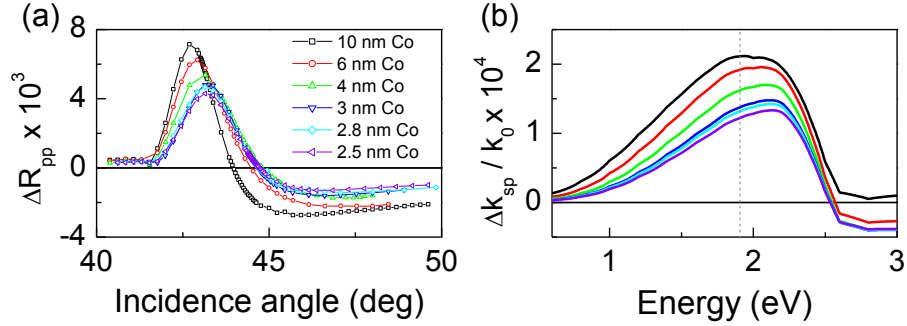


Fig. 4. (a) Transverse magneto-optical Kerr effect $\Delta R=R(+H)-R(-H)$ measured in the Kretschmann configuration for the Au(3 nm)/Co(d)/Au (20 nm) trilayers with d ranging from 2.5 to 10 nm. (b) Field dependent variation of the SPP wave vector $\Delta k_{sp}=k_{sp} (+H)-k_{sp} (-H)$. The dashed line represents the energy of the radiation used in the measurements $E=1.96$ eV.

To continue our discussion on the magneto-optical properties of the trilayers, we consider that the transverse MOKE signal is typically expressed as the normalized variation in reflectivity of the p -polarized light:

$$\frac{\Delta R_{pp}}{R_{pp}} = \frac{R_{pp}(+H) - R_{pp}(-H)}{R_{pp}(0)} \quad (1)$$

The magnitude of this ratio might be misleading in systems illuminated in the Kretschmann configuration since the reflectivity tends to zero in optimized samples whereas the field dependent variation of the reflectivity does not. Nevertheless, this ratio can be used in sensing applications as previously demonstrated [2,10], because the sensitivity is strongly enhanced when the critical thickness is achieved. Figure 5 shows $\Delta R_{pp}/R_{pp}$ measured for the Au(3 nm)/Co(d nm)/Au(20 nm) trilayers. A maximum value of $\Delta R_{pp}/R_{pp} \sim 3.2$ (relative variation of 320%) is found for the trilayer with $d=2.8$ nm, which is the highest value ever reported for this system to the best of our knowledge.

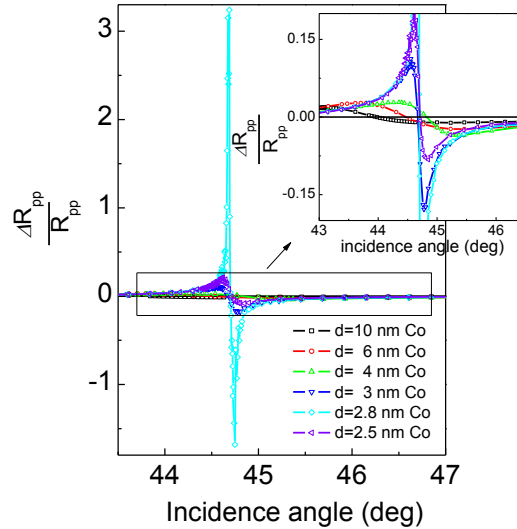


Fig. 5. Angular dependence of the relative variation in reflectivity $\Delta R_{pp}/R_{pp}$ for the Au(3 nm)/Co(d)/Au(20 nm) trilayers with d ranging from 2.5 to 10 nm. A maximum value of $\Delta R_{pp}/R_{pp} \sim 3.2$ (relative variation of 320%) is found for the trilayer with $d=2.8$ nm.

Once the critical thickness for this system was experimentally achieved, we analyzed the distribution and intensity of the EM fields within the samples. Hermann *et al.* [17] showed how the MO response of multilayers incorporating a magnetic thin layer is related to the intensity of the EM fields at the position of the magnetic layer. They showed that in the TMOKE geometry, the variation of the complex reflection coefficient for p -polarized light Δr_{pp} is directly proportional to the product of the TM electric field components (E_x and E_z) [20] within the magnetic layer, which along with H_y are the only EM fields present in TM modes. In the ultrathin film limit, where the electric fields can be considered constant within the magnetic film, the relationship is [17,28]:

$$\Delta r_{pp} = \frac{ik_0^2}{2\kappa_1 t} \varepsilon_{xy} l_m E_x E_z \quad (2)$$

where $k_0 = \omega/c$ is the wave number in vacuum, κ_1 is the z component of the incident light wave vector at the first interface, ε_{xy} are the MO constants of the magnetic film, l_m is the thickness of the magnetic film and t accounts for the absorption of such film [17]. Thus, by placing a MO active layer within the Au film and measuring the variation of the complex reflectivity it is possible to probe the actual intensity of the SPP generated EM fields at the location of the magnetic layer. We used this method to study the intensity and spatial distribution of the SPP generated electromagnetic fields. For this study we prepared Au/Co/Au trilayers with critical thickness (25.8 nm) and with a 2.8 nm thick Co layer positioned at different distances from the upper air-Au interface as shown in Fig. 6. Reflectivity and MO measurements in different configurations were carried out in order to extract the change in the complex reflection coefficient Δr_{pp} when an external magnetic field is applied as shown in Ref [17]. For this we used p polarized light [Fig. 6(a)], light rotated 45° from the p -axis and with a polarization analyzer oriented at 45° [Fig. 6(b)], light rotated 45° from the p -axis and with a quarter wave plate with its fast axis along p followed by a polarization analyzer oriented at 45° [Fig. 6(c)] and s -polarized light [Fig. 6(d)]. Thus, the left column in Fig. 6 shows the reflectivity vs. incidence angle in the different configurations whereas the right column displays the MO response in each case. No MO response is obtained with s polarized light. In spite of the fact that all the samples have the same total Au and Co thickness, slight variations in the reflectivity curves are found due to slight modification of the excitation conditions of the SPPs by inserting a Co film in different positions.

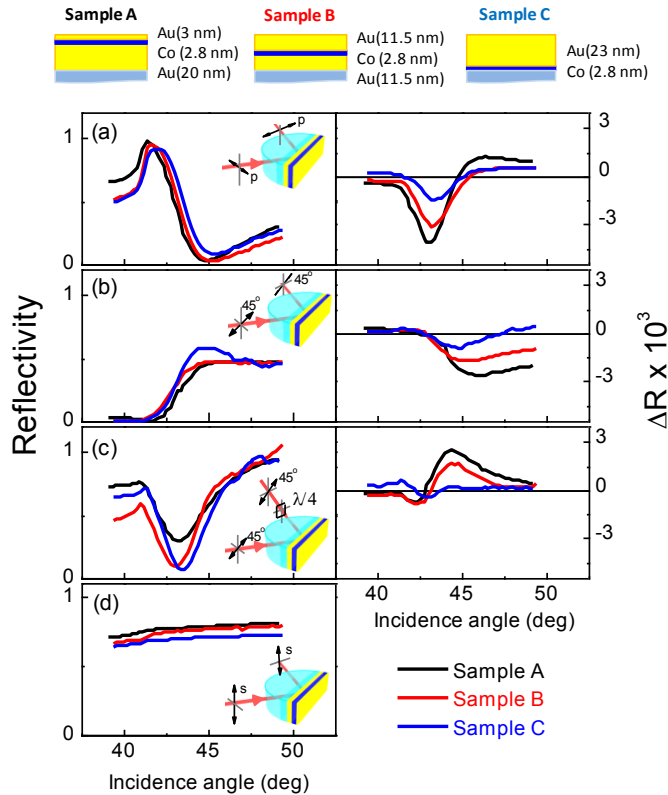


Fig. 6. (Color online) Variation with the incidence angle of the reflectivity (left column) and MO response (right column) for the Au/Co/Au trilayers with Co positioned at 3 nm (up), 11.5 nm (middle) and 23 nm (down) to the upper air-Au interface using (a) *p*-polarized light, (b) light rotated 45° from the *s* (and *p*) axis and a polarization analyzer oriented at 45°, (c) same as (b) but inserting a quarter wave plate with its fast axis along *p* and (d) using *s*-polarized light.

The variation of the complex reflection coefficient Δr_{pp} and thus the product of the TM electric field components (E_x and E_z) as a function of the position within the Au films can be obtained using the experimental data in Fig. 6, as described in Ref [17]. Figure 7(a), shows the measured $E_x E_z$ fields when positioning the Co film at different distances to the upper Au-air interface, normalized to the incident radiation. The results show the expected SPPs generated EM fields exponential decay as the distance to the upper Au-air interface increases. The EM field at the Au-air interface can be calculated using these results and taking into account the exponential decay of the $E_x E_z$ product and the difference between the dielectric constants of Au and Co that affect the E_z component. The calculated intensity of the EM field at the upper interface is shown with a dashed line in Fig. 7(a), exhibiting a normalized $E_x E_z$ value around 0.43 at the critical angle when SPPs are excited, compared to a much lower value of 0.1 expected for single Co films of critical thickness. Our experimental results are in good agreement with the EM field intensity simulations for Co layers at different positions within the trilayers [Fig. 7(b)]. Thus, we have demonstrated experimentally that for tailored trilayers with total critical thickness and a thin Co layer placed close to the air-metal interface, namely Au(3 nm)/Co (2.8 nm)/Au (20 nm)/glass, very high SPP-generated EM fields are achieved while keeping high sensitivity to externally applied magnetic fields.

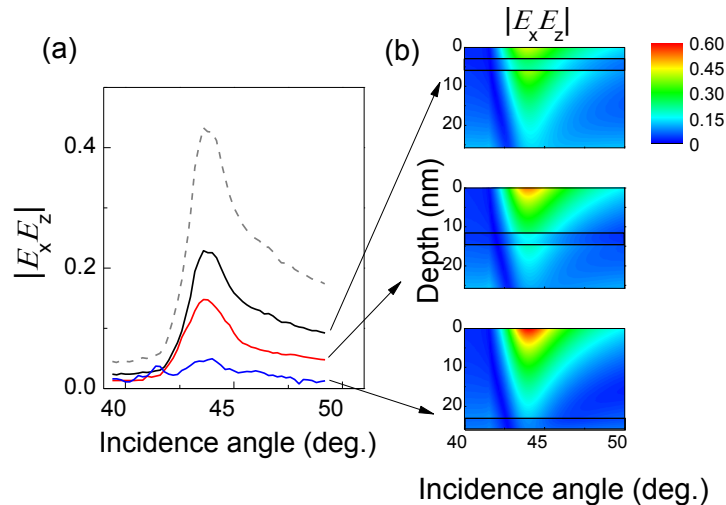


Fig. 7. (Color online) (a) Modulus of the product of the TM electric components $E_x E_z$ normalized to the incident intensity at the position in which the ferromagnetic film is placed in each case for the Au/Co/Au trilayers with Co positioned at 3 nm (up), 11.5 nm (middle) and 23 nm (down) to the upper Au-air interface. The dashed line represents the estimated value of $E_x E_z$ at the air-metal interface. (b) $E_x E_z$ is represented as a function of incidence angle and distance to the upper Au-air interface.

Conclusions

We have demonstrated that it is experimentally possible to achieve SPP modes in tailored Au/Co/Au trilayers that exhibit large electromagnetic fields that can also be modulated by externally applied magnetic fields. The MO activity, associated with the modification of the k_{sp} , exhibits a strong dependence with the external magnetic fields. By using magneto-optics as a tool, we have analyzed the field-dependent optical response in tailored Au/Co/Au trilayers and have been able to probe the SPP generated electromagnetic fields within the structures, checking them against simulated values calculated using transfer matrix formalism. Our studies are useful for the design of magneto-plasmonic components for varied applications based on leaky modes in SPP excitation.

Acknowledgements

This work was supported by DARPA (Grant # HR0011-07-1-0003 “Novel Sensors for Chemical and Biodefense”).